Hindawi Publishing Corporation
Journal of Nanotechnology
Volume 2012, Article ID 512738, 10 pages
doi:10.1155/2012/512738

Review Article

Study of Carbon Nanotube-Substrate Interaction

Jaqueline S. Soares and Ado Jorio

Departamento de Física, Universidade Federal de Minas Gerais, 31270-901 Belo Horizonte, MG, Brazil

Correspondence should be addressed to Jaqueline S. Soares, jssoares@fisica.ufmg.br

Received 13 July 2011; Accepted 27 September 2011

Academic Editor: Angel Berenguer

Environmental effects are very important in nanoscience and nanotechnology. This work reviews the importance of the substrate in single-wall carbon nanotube properties. Contact with a substrate can modify the nanotube properties, and such interactions have been broadly studied as either a negative aspect or a solution for developing carbon nanotube-based nanotechnologies. This paper discusses both theoretical and experimental studies where the interaction between the carbon nanotubes and the substrate affects the structural, electronic, and vibrational properties of the tubes.

1. Introduction

Nanotechnology has attracted broad interest in the society. Nanomaterials are unusual because of size-related effects and strong dimensionality dependence, leading to fascinating novel effects in their physicochemical properties. Carbon nanotubes are highly stable nanosystems due to the strong covalent bonds between the carbon atoms on the nanotube structure, being considered a model system for nanoscience [1]. Together with the stability, their unique structural, chemical, mechanical, thermal, optical, optoelectronic, and electronic properties are responsible for the interest in the fundamental properties of carbon nanotubes, so that their potential to applications continues to increase [2–4].

When moving into real applications, it is very important to consider the effect of the environment surrounding the nanostructure [1]. This work is devoted to how carbon nanotube properties can be affected by the presence of the substrate where the tube is sitting. The interactions between carbon nanotubes and the substrate have been widely studied as a drawback or a solution for the development of nanotechnologies based on carbon nanotubes [5–30].

The challenge to use carbon nanotubes is the formation of organized arrangements that are technologically important. Recent advances have been achieved by controlling the shape and organization of nanotubes on surfaces [23, 26–29, 31, 32]. Such manipulation offers the possibility of designing and building a wide range of nanoelectronic devices. In this case, the structural and electronic properties of carbon nanotubes, considering the interaction with substrates in which they are deposited, are crucial for applications. In fact, recent studies have shown that a strong interaction between carbon nanotubes and the substrate can lead to important changes in the nanotube properties. For example, single-wall carbon nanotubes (SWNTs) deposited on quartz gives rise to a superlattice of semiconductor and metal system, where the conduction behavior depends on the orientation between the tube and the substrate [30]. That is, the tube and the substrate are actually a new system that cannot be considered as only the sum of tube plus substrate.

This paper is organized as follows. Section 2 provides a summary of the effects related to substrate-induced tube flattening and distortion; Section 3 presents how environmental conditions change the optical transition energies (E_{ii}) and vibrational properties, focusing on the radial breathing mode (RBM) frequency (ω_{RBM}); Section 4 discusses tube-substrate bonding; Section 5 discusses the substrate-induced superlattice formation; Section 6 discusses the effects on bundled and multiwalled tubes; finally, in Section 7 the conclusions are presented.

2. Tube Flattening and Distortion

First-principle calculations show that the tube flattening (see Figure 1), which can appear when the tube is sitting

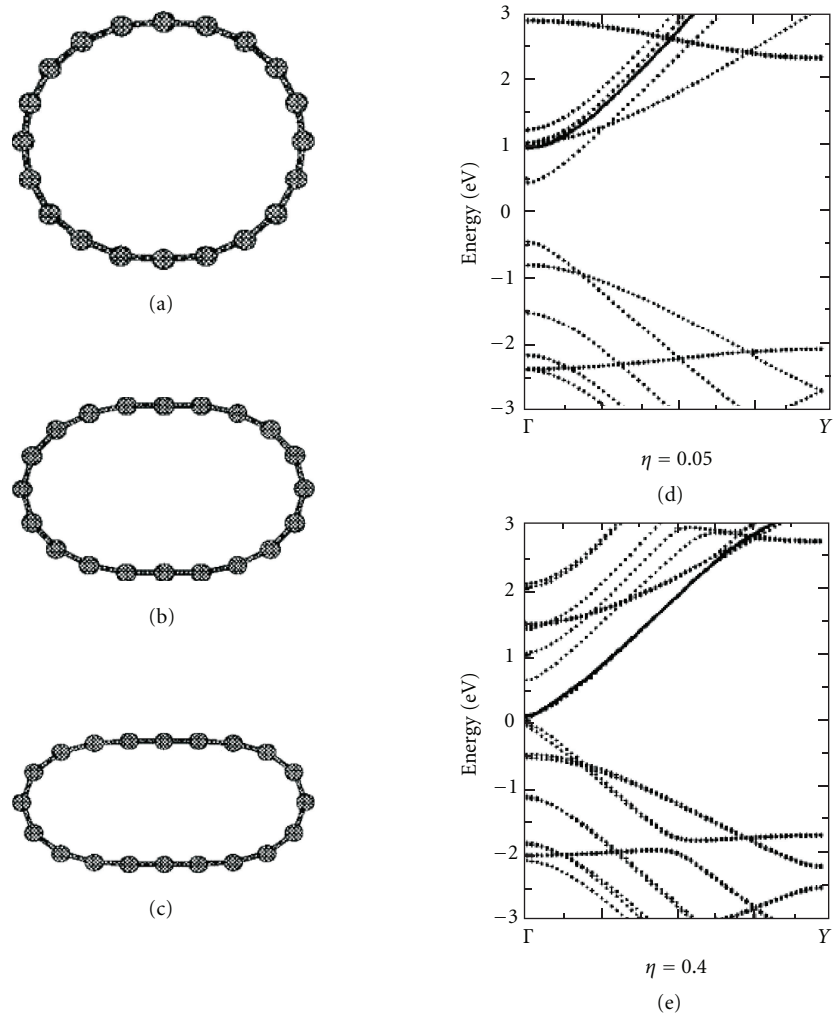

Figure 1: Relaxed cross-sections (a) of (10,0) carbon nanotubes with different degrees of flattness in (b) and (c). (d) and (e) plot the electronic band structures for a flattened (10,0) nanotube. The flatness is characterized by η which is defined as $\eta = (D_0 - d)/D_0$, where D_0 is the original diameter of the nanotube and d is the distance between two straight lines of the cross-section (adapted from [13]).

on a substrate, induces a semiconductor-metal transition. Such transition can be understood in terms of hybridization effects induced by the curvature [13], the flattening causing a progressive reduction of the band gap [13]. The tip of an atomic force microscope (AFM) can be used to control the shape and position of carbon nanotubes dispersed on a surface, and the interaction between nanotubes and the surface is crucial for such manipulations [31, 33]. The nanotubes tend to distort so as to conform to the topography of the substrate. Such distortions can have implications for the electronic structure and electrical transport properties of nanotubes [31]. Carbon nanotube is more strongly adhered to the substrate when the H atoms between the tube and the substrate are removed [22], thus making it difficult to disturb the tube with the AFM tip, for example. On the fully hydrogenated silicon surface, the electronic structure of a metallic carbon nanotube is almost unchanged. Removing partially the H atoms from the adsorption site, there is an enhancement in the metallicity of the system. However, when all the H atoms are removed, the system becomes a semiconductor [19, 20]. Stronger interaction between the carbon and surface atoms might also occur, and this subject will be discussed in Section 4.

3. E_{ii} and ω_{RBM}

The Raman spectroscopy has been widely used for characterizing SWNTs [8, 34, 35]. The mapping technique based on the Raman spectroscopy makes it possible to study local environmental effects of the Raman features from one single SWNT. For example, effects introduced by the substrates can be studied through comparative Raman lineshape studies of SWNTs freely suspended crossing tranches versus sitting on substrates [7, 11, 36–38]. The Raman spectra variations observed in these works can be attributed to nanotube-substrate interactions.

The RBM can be used to study the nanotube diameter (d_t) through its frequency (ω_{RBM}), to probe the electronic

structure through its intensity (I_{RBM}) and to perform an (n, m) assignment of a single isolated SWNT from analysis of both d_t and I_{RBM} [8, 34, 35, 42]. The Kataura plot [39] shows the optical transition energies (E_{ii}) for each (n, m) SWNT as a function of ω_{RBM}. Figure 2 [39, 40, 43, 44] shows E_{ii} ranging from E_{11}^S up to E_{66}^S (S stands for semiconducting tube and M stands for metallic tubes). Figure 2(a) uses the standard relation $\omega_{\mathrm{RBM}} = 227/d_t$ [40], and the E_{ii} values were obtained using the empirical equation [44]:

$$E_{ii}(p, d_t) = 1.074(p/d_t)\left[1 + 0.467\log(0.812 d_t/p)\right] + \beta_p \cos 3\theta/d_t^2, \quad (1)$$

where p is defined as $1, 2, 3, \ldots, 8$ for $E_{11}^S, E_{22}^S, E_{11}^M, \ldots, E_{66}^S$, respectively, and the values of β can be found in [44].

For SWNTs on top of crystalline miscut quartz, there is a strong environmental effect related to the tube-substrate interaction [41], although the RBM frequencies are homogeneous along the whole SWNTs. The (n, m) assignment for the observed RBMs (up triangles in Figure 2(a)) cannot be performed using the standard Kataura plot because several up triangles fall in regions where there are no corresponding E_{ii} values from any (n, m) SWNT (no matching between triangles and circles). For RBM-based (n, m) identification, it is important to find out how various environmental conditions change the optical transition energies (E_{ii}) and the ω_{RBM} values [40, 41, 43–45]. Figure 2(b) shows the matching between the Kataura plot and many RBM Raman data for the SWNTs on crystalline miscut quartz [41]. For this (n, m) assignments, two parameters (E_{ii} and C) can be changed to adjust in the Kataura plot: (i) the carbon nanotube-substrate interaction exhibits a $\omega_{\mathrm{RBM}}(d_t)$ relation according to the following equation [40]:

$$\omega_{\mathrm{RBM}} = (227/d_t)\sqrt{1 + C * d_t^2}, \quad (2)$$

with $C = 0.082 \pm 0.009\,\mathrm{nm}^{-2}$ and (ii) a downshift of $\Delta E_{ii} = -100 \pm 30\,\mathrm{meV}$ in E_{ii} with respect to the standard values [44, 45]. These results suggest a strong interaction between carbon nanotube and crystalline quartz substrate as compared to other types of samples, since ΔE_{ii} and C are the largest values among different tube-environment systems analyzed in the literature [40, 41, 44, 45].

It is important to remember that the experimental results in the literature have been fitted with the relation $\omega_{\mathrm{RBM}} = \mathbf{A}/d_t + \mathbf{B}$, instead of (2), with the values for **A** and **B** varying from paper to paper [45]. However, Araujo et al. showed that all the results between ω_{RBM} and d_t found in the literature can be described by (2), with the advantage that C is the only adjustable constant, weighting the effect of the different medium surrounding the SWNT samples [40, 41, 44, 45].

4. Tube-Substrate Bonding

4.1. Semiconductor-Metal Transition. Stronger interactions between carbon nanotubes and the surface can occur. The most commonly used substrate is silicon substrate [14, 19–21]. The formation of Si–C bonds enhances the metallic character of the nanotube by the contact with the Si surface [14]. The electronic properties of the adsorbed tubes are also sensitive to the carbon nanotube adsorption sites. The structure is semiconducting when the adsorbed carbon nanotube is perpendicular to the Si dimers, while it is metallic when the nanotube is parallel to the Si dimers [21].

Another substrate studied is a quartz substrate. Among the substrates used to study the interaction of carbon nanotubes with the substrate, the quartz was identified as a promising substrate for the growth of complex structures of SWNT [23, 26–29]. An interesting carbon nanotube structure was grown on quartz substrate, the so-called SWNT serpentine, which consists of a series of straight, parallel, and regularly spaced segments, connected by alternating U-turns [23]. The formation of these structures can be explained by the mechanism called "falling spaghetti" [23, 46]. This structure provides a great deal of information because the same SWNT exhibits different interactions due to the tube-substrate morphology [30]. The first-principles calculations shown in Figure 3 stand for SWNT serpentine placed on top of a crystalline quartz [30]. Upon relaxation, the silicon atoms in the contact region are found to experience an upward displacement and the bottom part of the nanotube becomes flat, resulting from a strong interaction between carbon bonding states and surface dangling bonds [30]. While Figure 3(a) shows the electronic structure of an original semiconductor (19,0) nanotube, Figure 3(b) shows the results of this same (19,0) tube, but now interacting with a SiO_2 slab having Si dangling bonds (see insets to Figure 3). The existence of a periodic array of interaction sites causes the appearance of dispersive bands crossing the Fermi level (red rectangle in Figure 3(b)), showing the semiconductor-metal transition [30]. The next sections present experimental evidence about these substrate effects.

The interaction of carbon nanotubes with other substrates has also been studied [7, 17, 23–29], for example, InAs substrate. First-principle calculations were used to study the binding mechanisms for zigzag carbon nanotubes on InAs substrate. Nanotubes preferentially bind to surface in atoms, while maintaining their own internal structural and electronic integrity [17].

4.2. Experimental Evidence for Metal-Semiconductor Transition for SWNTs on Quartz. The G band Raman frequency depends sensitively on strain [47–49] and doping [50–52]. When the tube becomes metallic, the Kohn anomaly appears for the longitudinal optical (LO) phonon, which decreases and broadens the peak [51, 53]. In addition, frequency shifts of the dominant second-order mode (G′ band, at 2600–2700 cm^{-1}) can also be used to differentiate between electron donor (n) and acceptor (p) doping, even at the individual single-atom doping level [54]. These aspects of the Raman spectroscopy are exemplified in the two representative Raman spectra shown in Figure 4. The frequency behavior for both the G and G′ bands is a method to characterize the strain [47–49] and doping [50–52] induced by the tube-substrate interaction and to understand the observation of a mixed metal-semiconductor behavior (see spectrum in Figure 4(b)).

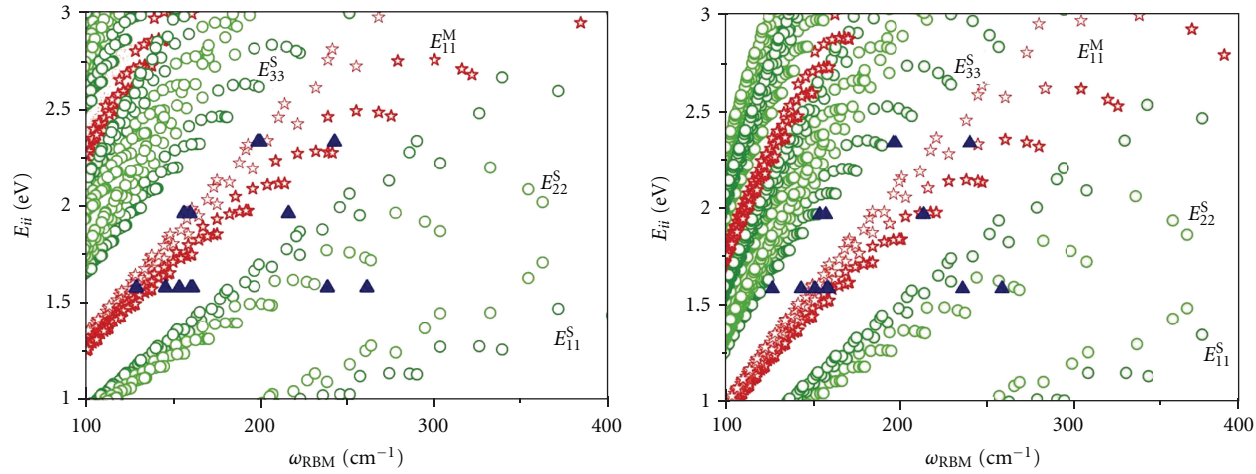

FIGURE 2: Optical transition energies (E_{ii}) of each (n, m) SWNT plotted versus the respective RBM frequencies (ω_{RBM}), known as the Kataura plot [39]. The optical transition energies of semiconducting (circles) and metallic (stars) SWNTs are shown. Up triangles represent RBM results obtained from resonance Raman spectroscopy, taken from SWNTs deposited on crystalline miscut quartz [23]. The y-axis for these up triangles coordinates is chosen by considering resonance at $E_{ii} \approx E_{laser}$. The x-axis is chosen by considering a correspondence between ω_{RBM} and d_t: (a) the standard relation $\omega_{RBM} = 227/d_t$ [40], and E_{ii} from (1); (b) Equation (2) with $C = 0.082\,\text{nm}^{-2}$ and a 100 meV downshift in E_{ii} with respect to the values in (a) (adapted from [41]).

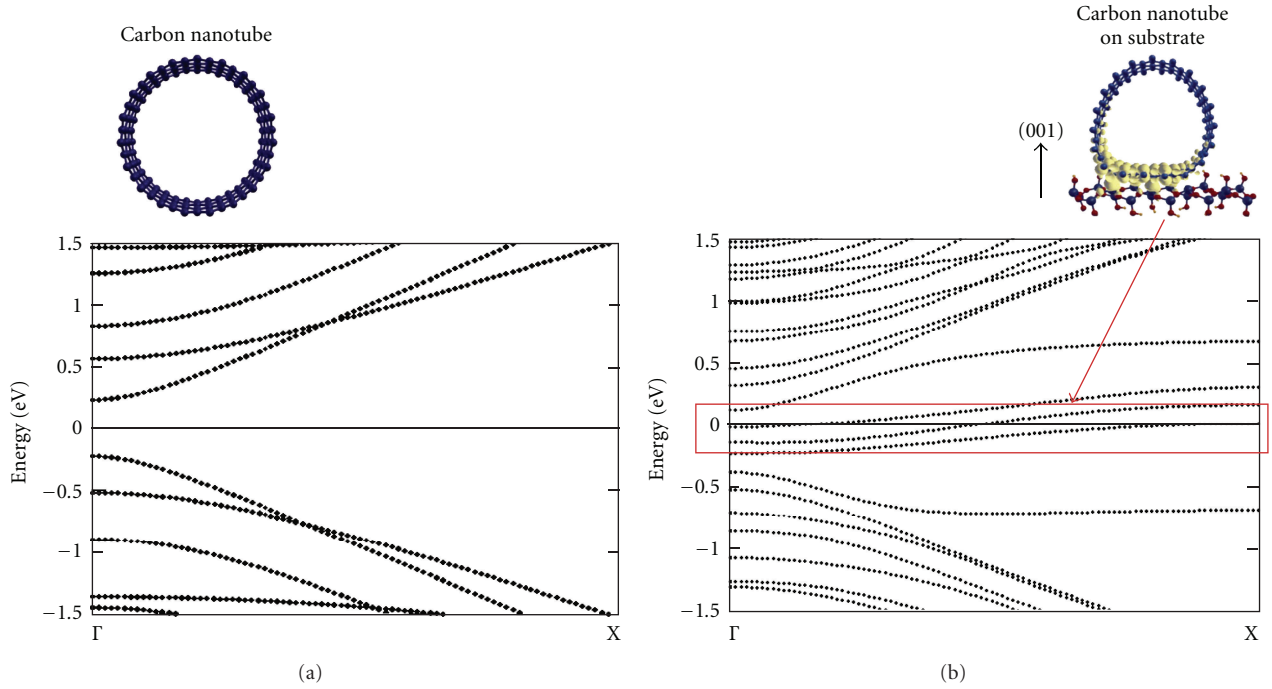

FIGURE 3: Band structure of the (19,0) carbon nanotube: (a) pristine and (b) interacting with a (001) surface of a quartz substrate with tube axis along (100). The Fermi level is set to zero. The insets show the respective atomic structures. The yellowish clouds in the inset (b) represent a plot of the electronic density for states within energies of up to 0.1 eV around the Fermi level (red rectangle in (b)). The bands responsible for the gap closure are localized spatially in the contact region along the flat surface of the nanotube (adapted from [30]).

Figures 4(a) and 4(b) show two G band Raman spectra from the same SWNT deposited on crystalline quartz. The difference is that (a) is located at a serpentine segment where the tube-substrate interaction is weak, while (b) is located at a serpentine segment where the tube-substrate interaction is strong. The G band features in spectrum (a) are typical of a semiconducting SWNT [8], while the G band features in spectrum (b) show a sum of metal and semiconductor behavior. The change in the G band profile indicates a metallic versus semiconductor character, with

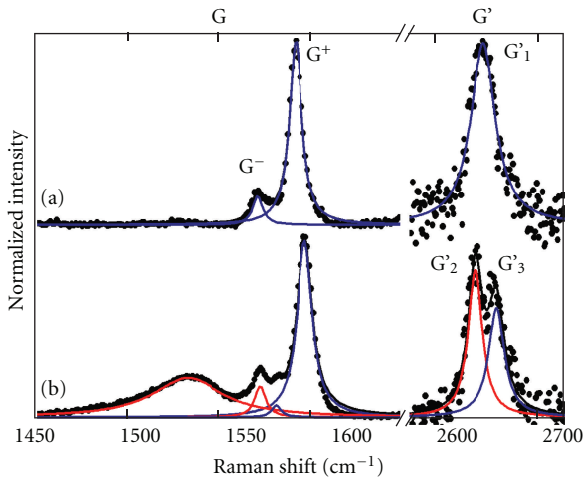

FIGURE 4: Raman spectroscopy analysis of one SWNT grown on quartz. Spectrum (a) exhibits a G band with a line shape typical of a semiconducting SWNT. Spectrum (b) exhibits a G band showing a mixture of lineshapes typical of semiconducting (blue Lorentzians) and a metallic (red Lorentzians) SWNT behavior. Note that the G′ peak splits in (b) (adapted from [30]).

an additional broad peak at the G band in 1530 cm^{-1} due to the Kohn anomaly [53]. Spectrum (a) shows a G′ band with a single peak, while spectrum (b) shows a splitting of the G′ band. The shifts in the G′ band features can be explained by doping, which can cause either an upshift or downshift due to doping, according to [54]. The G and G′ bands spectra are different, clearly related to the morphology, that is, tube segments aligned and not aligned along the steps of the crystalline miscut quartz substrate. Points located at the portions of the SWNT crossing the quartz atomic steps exhibit only one G′ peak and two G band peaks characteristic of semiconducting SWNTs (Figure 4(a)). Points where the nanotube lies along to the substrate atomic steps exhibit two G′ peaks (see spectrum (b) in Figure 4), and the G band exhibits four peaks (two characteristic of a semiconducting SWNT—blue Lorentzians in spectrum (b) of Figure 4 — and two characteristic of a metallic SWNT — red Lorentzians in spectrum (b) of Figure 4).

4.3. Nonhomogeneous SWNT-Substrate Interactions. As we have seen, the substrate changes the G band behavior. However, the substrate does not affect all nanotubes in the same way; that is, the SWNT may show different interactions with the substrate indicating nonhomogenous interaction. In the case discussed in Figure 4, the ω_{G+} is observed to oscillate according with the tube-substrate morphology [30]. The frequency variation can be explained by the stronger strain [47–49] and doping [50–52] in the flat segments, corroborating the stronger versus weaker modulated tube-substrate interaction when the nanotube lies along versus across the substrate surface steps [30].

In general, the G^+ band behavior for SWNT serpentines grown on crystalline quartz can be separated in three groups: (i) frequency has its maximum value at the center of straight segments along the steps and minimum at the center of the U-shaped segments—this is the case discussed in Figure 4 [30] and shown in Figure 5(a) for another SWNT serpentine [55]; (ii) frequency changes very little (Figure 5(b)), indicating very weak or no tube-substrate interaction [55]; (iii) frequency "jumps" at certain points in the SWNT serpentine (Figure 5(c)), indicating a very strong and localized perturbation [55]. These effects can be generally understood as a result of different types of interaction with the substrate, generated during the synthesis of SWNT serpentines [46] and local aspects, such as impurities and local charging [30, 55].

5. Superlattice Formation

5.1. The Raman Spectroscopy. As shown in Section 4.2, the G-band frequency (ω_G) can be used to distinguish between metallic and semiconducting SWNTs, through strong differences in their Raman lineshapes [35, 56]. Figure 6(a) shows a spectroscopic confocal image of a SWNT serpentine. Figure 6(b) gives a general view of the G band Raman spectra of the carbon nanotube at the 1–5 locations from the single-wall carbon nanotube shown in Figure 6(a), taken along the serpentine. Regions 1, 3, and 5 in Figure 6(a) were taken at the flat segments of the SWNT serpentine, which are strongly attached to the quartz substrate, thus exhibiting strong tube-substrate interaction. When the tube goes down the steps (regions 2 and 4 in Figure 6(a)), the interaction is weak. The appearance and disappearance of the lower frequency G^- feature (~1540 cm^{-1}), related to the tube-substrate morphology and interaction, show that the periodic change on the tube-substrate interaction generates a set of alternate metal-semiconductor tube segments, that is, a superlattice formation [30].

5.2. Electric Force Microscopy (EFM). Electric force microscopy (EFM) has been shown to differentiate metal and semiconducting SWNTs [57], and it was used to corroborate the Raman results for the superlattice formation. Figure 7 provides a schematic for understanding the metal versus semiconductor EFM behavior. The EFM measures the dielectric response of the whole sample, that is, SWNT plus substrate. In general, when the tip approaches the dielectric material, there is a decrease in $\Delta\omega$. Then two effects happen in our measurement, as depicted in Figure 7: (1) $\Delta\omega$ decreases when the tip approaches the tube, reaches a minimum when at the top of the tube, and increases back when the tip departs from the tube (see column (a) in Figure 7); (2) $\Delta\omega$ shows a slight increase during the constant-height scan, because the EFM tip retracts when crossing the tube (see column (b) in Figure 7), and the change in surface-tip distance causes a lowering in the tip-substrate interaction. The overall result is a sum of these two effects (see column (c) in Figure 7). In the case of semiconducting SWNT (blue), when the EFM tip is going on top of the tube, the tip retraction due to change in surface height causes a lowering in the tip-substrate interaction, giving rise to the "W shaped" in the semiconducting SWNTs. This effect is indeed present in the metallic SWNT (red), but due to the stronger and

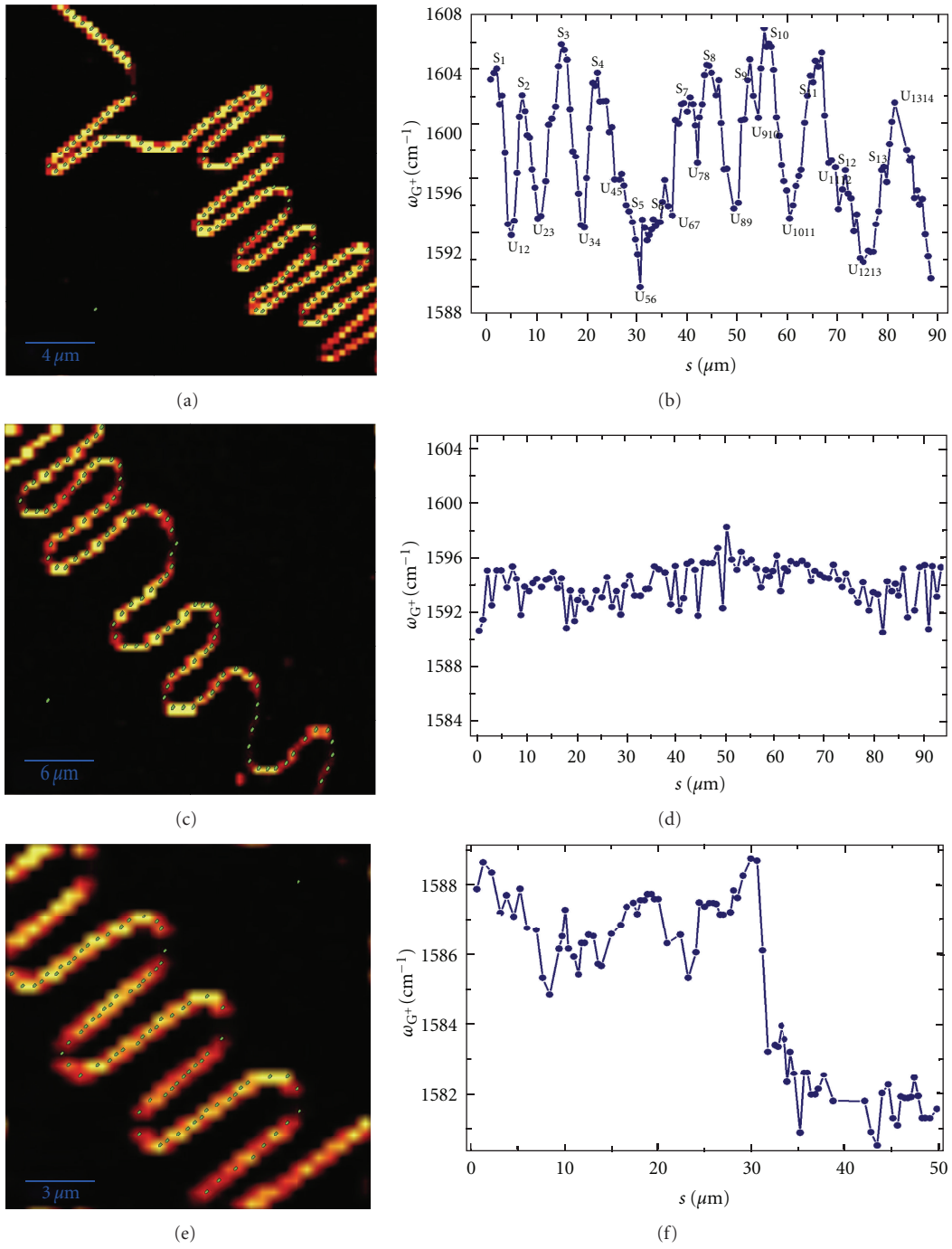

FIGURE 5: (a), (c), and (e) show spectroscopic images of G band of SWNT serpentines on quartz substrate, using the excitation laser wavelength of 532 nm (E_{laser} = 2.33 eV). (b), (d), and (f) show the G^+ frequency of these SWNTs, observed in all points indicated by green pointers in (a), (c), and (e), respectively, plotted as a function of the distance s, measured along the SWNT: (b) frequency has maximum and minimum following the tube-substrate morphology (a); (d) variation in frequency within experimental accuracy; (f) frequency "jumps" [55].

sharper dielectric response, it shows just a slight distorter "V-shaped" EFM profile [30].

Figure 8 shows the EFM analysis of the same SWNT discussed in Figure 6. The EFM measurements (Figure 8) for a SWNT serpentine placed on top of a crystalline quartz substrate support the superlattice formation (mixed metal-semiconducting character) observed in the Raman spectroscopy [30]. Even though the EFM signal seems homogeneous in Figure 8(a), a more careful analysis reveals structure in this line shape, as shown in the line profiles across two different regions in the nanotube presented in Figure 8(b). The red and blue profiles correspond to the regions marked

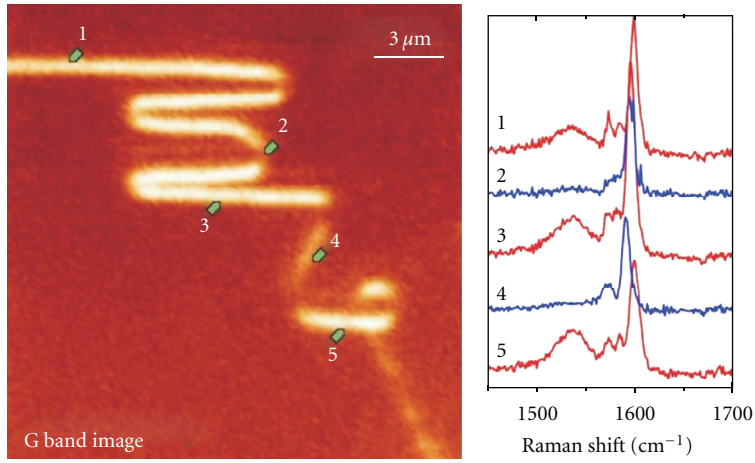

FIGURE 6: (a) Confocal image of the G band integrated intensity (E_{laser} = 1.96 eV, spatial resolution ~500 nm) for SWNT serpentine on (1 $\bar{1}$ 0 1) quartz. The spectral intensity is stronger in segments aligned along the steps because of the light polarization dependence for the Raman scattering [8]. (b) The G band at different points on the same serpentine shown in (a). An additional broad peak at the G band (~1540 cm^{-1}) has been observed on the flat sections (spectra 1, 3, and 5), indicating a metallic character. This additional peak disappears in spectra 2 and 4, indicating a semiconducting character (adapted from [30]).

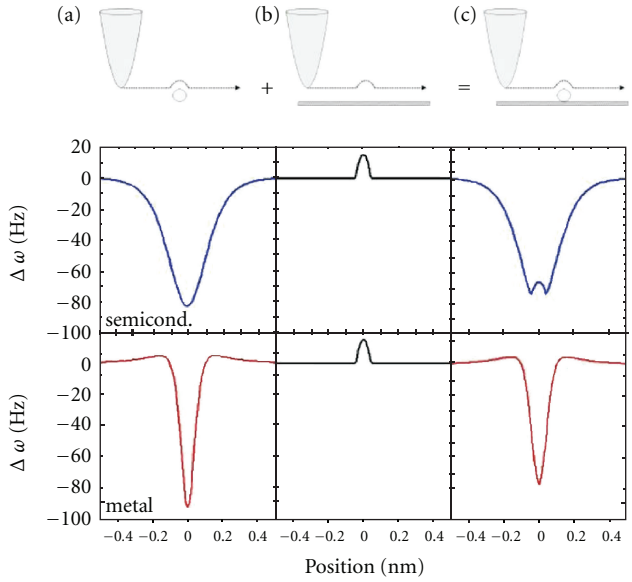

FIGURE 7: The EFM profiles for semiconducting and metallic SWNTs. In column (a), the effect of the EFM tip crossing a semiconductor (blue) and a metallic (red) SWNTs on $\Delta\omega$ is shown. The lineshapes are different due to the differences in dielectric response. In column (b) the effect of the EFM tip retracting from the substrate on $\Delta\omega$ is shown. Here the effect is the same for both semiconductors and metals. In column (c) the two effects are combined. The equations in [57] were used to build these plots [30].

by the red and blue lines in Figure 8(a), respectively. The "W-shaped" blue profile, typical for a region with weak substrate interaction, is the EFM signature for a semiconducting nanotube [57], whereas the "V-shaped" red profile, typical for a strong substrate interaction region, attests for a metallic behavior at this region of the SWNT, and these profiles corroborate the metal-semiconducting alternating behavior of SWNT serpentine Raman spectra.

It is important to comment that we expect the strong interaction between tube and crystalline quartz substrate reported here to be related to the presence of dangling bonds in the substrate; at the temperature of nanotube growth, the surface contains exposed unpassivated Si atoms [30]. The same SWNT might behave differently if deposited on the same quartz substrate at room temperature, since the Si atoms are expected to be passivated in this case. More generally, nanotube-substrate interaction could change depending on how the system is made.

6. Substrate Interaction on Bundled and Multiwalled Tubes

Although the literature is poor on this subject, for completeness we now discuss the substrate effect on two more complex systems, which are single-wall carbon-nanotube bundles and carbon nanotubes with more than one wall.

The properties of SWNT bundles can also be affected when the bundles are deposited on a substrate, with the additional complication that the structural and electronic properties of the tubes themselves change due the tube-tube interaction [58–60]. Rao et al. [59] showed a parameterized calculation of isolated and bundled armchair nanotubes using the method of Kwon et al. [58]. They observed differences in the density of states in isolated and bundled tubes, an increase in the separation of the valence, and conduction-band singularities, which is in contrast with the results found by Reich et al. [60]. When bundled nanotubes are deposited on a substrate, the tube-tube interaction could affect the electronic changes due to the tube-substrate interplay.

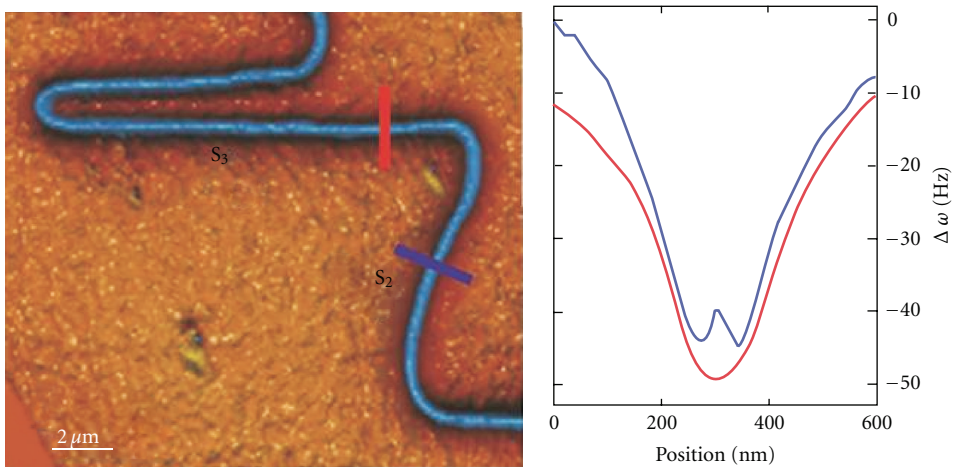

Figure 8: (a) Electric force microscopy (EFM) image of the same SWNT serpentine discussed in Figure 6. (b) Scanning across the SWNT, the cantilever frequency shift is different if a tube is semiconducting ("W shaped" blue line) or metallic ("V shaped" red line) [57]. The red and blue lines in (a) indicate the two regions where these profiles in (b) were acquired [30].

Considering now carbon nanotubes with more than one concentric wall (double-walled, triple-walled, or multiwalled carbon nanotubes), the higher complexity resides on the environmental effects affecting the inner and outer walls differently, summed with the tube-tube interactions. Villalpando-Paez et al. [61] showed that the (*6,5*) inner tubes in a double-wall carbon nanotube (DWNT) show different behavior when surrounded by different (n, m) outer tubes. The extra effect of a substrate in this case is a broad and open issue for future research.

7. Conclusions

In this paper, the importance of the substrate in carbon nanotube properties has been discussed. SWNTs are candidates for sensing applications, since interactions with the surface are the basis for sensing, while in SWNTs every carbon atom is on the surface [4]. Properties of SWNTs are affected in several ways when the local environment changes. The strong interaction between the SWNT and the substrate generates measurable modifications on the electronic and vibrational structure, providing information about nanotube properties. The strong and weak interactions between SWNT and substrate can be studied in detail using the resonance Raman process, which has been widely used for characterizing SWNTs. The crystalline substrate strongly affects the RBM frequency and resonance energies. For making the (n, m) assignments for the SWNTs on substrate, it is necessary to adjust two parameters, E_{ii} and C, in the Kataura plot. The Raman spectra G and G′ bands can also be used to study nanotube-substrate interactions, including metal-semiconductor transition. The knowledge of these Raman signatures allows a detailed study of the environmental perturbations in SWNTs.

Finally, carbon nanoscience holds promise for a revolution in electronics at some point in the future [5]. New applications for nanocarbons, such as nanotubes, appear to hold promise as we look to the future, and we expect these applications to increasingly drive applied research in SWNTs. In particular, nanotube-substrate interaction is an important issue for reaching real applications.

Acknowledgments

J. S. Soares and A. Jorio acknowledge E. Joselevich, N. Shadmi, T. S. Yarden, A. Ismach, N. Geblinger, B. R. A. Neves, A. P. M. Barboza, M. S. C. Mazzoni, N. M. Barbosa Neto, L. G. Cançado, D. Nakabayashi, P. T. Araujo, E. B. Barros, C. Vilani, M. S. Dresselhaus, G. Dresselhaus, and L. Novotny, who contributed to the development of this work. The authors also acknowledge financial support from the Rede Nacional SPM Brasil, Rede Nacional de Pesquisa em Nanotubos de Carbono, INCT em Nanoestruturas de Carbono, MCT-CNPq, and AFOSR/SOARD (Award no.FA9550-08-1-0236).

References

[1] A. Jorio and M. S. Dresselhaus, "Nanometrology links state-of-the-art academic research and ultimate industry needs for technological innovation," *Materials Research Society Bulletin*, vol. 32, no. 12, pp. 988–993, 2011.

[2] A. Hirsch, *Fullerenes and Related Structures: Topics in Current Chemistry*, Springer, New York, NY, USA, 1998.

[3] R. H. Baughman, A. A. Zakhidov, and W. A. De Heer, "Carbon nanotubes—The route toward applications," *Science*, vol. 297, no. 5582, pp. 787–792, 2002.

[4] A. Jorio, G. Dresselhaus, and M. S. Dresselhaus, *Carbon Nanotubes: Advanced Topics in the Synthesis, Structure, Properties and Applications*, Springer, Berlin, Germany, 2008.

[5] P. Avouris, Z. Chen, and V. Perebeinos, "Carbon-based electronics," *Nature Nanotechnology*, vol. 2, no. 10, pp. 605–615, 2007.

[6] P. Avouris, M. Freitag, and V. Perebeinos, "Carbon-nanotube photonics and optoelectronics," *Nature Photonics*, vol. 2, no. 6, pp. 341–350, 2008.

[7] M. Steiner, M. Freitag, J. C. Tsang et al., "How does the substrate affect the Raman and excited state spectra of a carbon nanotube?" *Applied Physics A*, vol. 96, no. 2, pp. 271–282, 2009.

[8] M. S. Dresselhaus, G. Dresselhaus, R. Saito, and A. Jorio, "Raman spectroscopy of carbon nanotubes," *Physics Reports*, vol. 409, no. 2, pp. 47–99, 2005.

[9] A. Hartschuh, H. N. Pedrosa, J. Peterson et al., "Single carbon nanotube optical spectroscopy," *ChemPhysChem*, vol. 6, no. 4, pp. 577–582, 2005.

[10] T. Hertel, A. Hagen, V. Talalaev et al., "Spectroscopy of single- and double-wall carbon nanotubes in different environments," *Nano Letters*, vol. 5, no. 3, pp. 511–514, 2005.

[11] Y. Zhang, J. Zhang, H. Son, J. Kong, and Z. Liu, "Substrate-induced Raman frequency variation for single-walled carbon nanotubes," *Journal of the American Chemical Society*, vol. 127, no. 49, pp. 17156–17157, 2005.

[12] T. Hertel, R. E. Walkup, and P. Avouris, "Deformation of carbon nanotubes by surface van der Waals forces," *Physical Review B*, vol. 58, no. 20, pp. 13870–13873, 1998.

[13] M. S. C. Mazzoni and H. Chacham, "Bandgap closure of a flattened semiconductor carbon nanotube: a first-principles study," *Applied Physics Letters*, vol. 76, no. 12, pp. 1561–1563, 2000.

[14] W. Orellana, R. H. Miwa, and A. Fazzio, "First-principles calculations of carbon nanotubes adsorbed on Si(001)," *Physical Review Letters*, vol. 91, no. 16, pp. 1668021–1668024, 2003.

[15] C. Jiang, J. Zhao, H. A. Therese, M. Friedrich, and A. Mews, "Raman imaging and spectroscopy of heterogeneous individual carbon nanotubes," *Journal of Physical Chemistry B*, vol. 107, no. 34, pp. 8742–8745, 2003.

[16] V. V. Tsukruk, H. Ko, and S. Peleshanko, "Nanotube surface arrays: weaving, bending, and assembling on patterned silicon," *Physical Review Letters*, vol. 92, no. 6, pp. 655021–655024, 2004.

[17] Y. H. Kim, M. J. Heben, and S. B. Zhang, "Nanotube wires on commensurate InAs surfaces: binding energies, band alignments, and bipolar doping by the surfaces," *Physical Review Letters*, vol. 92, no. 17, p. 176102, 2004.

[18] A. Ismach, L. Segev, E. Wachtel, and E. Joselevich, "Carbon nanotube graphoepitaxy: highly oriented growth by faceted nanosteps," *Angewandte Chemie International Edition*, vol. 43, no. 33, pp. 11554–11555, 2004.

[19] R. H. Miwa, W. Orellana, and A. Fazzio, "Substrate-dependent electronic properties of an armchair carbon nanotube adsorbed on H/Si(001)," *Applied Physics Letters*, vol. 86, no. 21, Article ID 213111, pp. 1–3, 2005.

[20] S. Berber and A. Oshiyama, "Atomic and electronic structures of carbon nanotubes on Si(001) stepped surfaces," *Physical Review Letters*, vol. 96, no. 10, Article ID 105505, pp. 1–4, 2006.

[21] G. W. Peng, A. C. H. Huan, L. Liu, and Y. P. Feng, "Structural and electronic properties of 4 Å carbon nanotubes on Si(001) surfaces," *Physical Review B*, vol. 74, no. 23, p. 235416, 2006.

[22] P. M. Albrecht and J. W. Lyding, "Local stabilization of single-walled carbon nanotubes on Si(100)-2 × 1:H via nanoscale hydrogen desorption with an ultrahigh vacuum scanning tunnelling microscope," *Nanotechnology*, vol. 18, no. 12, Article ID 125302, 2007.

[23] N. Geblinger, A. Ismach, and E. Joselevich, "Self-organized nanotube serpentines," *Nature Nanotechnology*, vol. 3, no. 4, pp. 195–200, 2008.

[24] A. P. M. Barboza, A. P. Gomes, B. S. Archanjo et al., "Deformation induced semiconductor-metal transition in single wall carbon nanotubes probed by electric force microscopy," *Physical Review Letters*, vol. 100, no. 25, Article ID 256804, 2008.

[25] Y. You, T. Yu, J. Kasim et al., "Visualization and investigation of Si-C covalent bonding of single carbon nanotube grown on silicon substrate," *Applied Physics Letters*, vol. 93, no. 10, Article ID 103111, 2008.

[26] S. Jeon, C. Lee, J. Tang, J. Hone, and C. Nuckolis, "Growth of serpentine carbon nanotubes on quartz substrates and their electrical properties," *Nano Research*, vol. 1, pp. 427–433, 2008.

[27] J. Huang and W. Choi, "Controlled growth and electrical characterization of bent single-walled carbon nanotubes," *Nanotechnology*, vol. 19, no. 50, Article ID 505601, 2008.

[28] Y. Yao, X. Dai, C. Feng et al., "Crinkling ultralong carbon nanotubes into serpentines by a controlled landing process," *Advanced Materials*, vol. 21, no. 41, pp. 4158–4162, 2009.

[29] J. Xiao, S. Dunham, P. Liu et al., "Alignment controlled growth of single-walled carbon nanotubes on quartz substrates," *Nano Letters*, vol. 9, no. 12, pp. 4311–4319, 2009.

[30] J. S. Soares, A. P. M. Barboza, P. T. Araujo et al., "Modulating the electronic properties along carbon nanotubes via tube-substrate interaction," *Nano Letters*, vol. 10, no. 12, pp. 5043–5048, 2010.

[31] T. Hertel, R. Martel, and P. Avouris, "Manipulation of individual carbon nanotubes and their interaction with surfaces," *Journal of Physical Chemistry B*, vol. 102, no. 6, pp. 910–915, 1998.

[32] P. Avouris, T. Hertel, R. Martel, T. Schmidt, H. R. Shea, and R. E. Walkup, "Carbon nanotubes: nanomechanics, manipulation, and electronic devices," *Applied Surface Science*, vol. 141, no. 3-4, pp. 201–209, 1999.

[33] M. R. Falvo, G. J. Clary, R. M. Taylor et al., "Bending and buckling of carbon nanotubes under large strain," *Nature*, vol. 389, no. 6651, pp. 582–584, 1997.

[34] A. Jorio, M. S. Dresselhaus, R. Saito, and G. Dresselhaus, *Raman Spectroscopy in Graphene Related Systems*, Wiley-VCH, Weinheim, Germany, 2011.

[35] A. Jorio, M. A. Pimenta, A. G. Souza Filho, R. Saito, G. Dresselhaus, and M. S. Dresselhaus, "Characterizing carbon nanotube samples with resonance Raman scattering," *New Journal of Physics*, vol. 5, pp. 139.1–139.17, 2003.

[36] H. Son, Y. Hori, S. G. Chou et al., "Environment effects on the Raman spectra of individual single-wall carbon nanotubes: suspended and grown on polycrystalllne silicon," *Applied Physics Letters*, vol. 85, no. 20, pp. 4744–4746, 2004.

[37] Y. Zhang, H. Son, J. Zhang, M. S. Dresselhaus, J. Kong, and Z. Liu, "Raman spectra variation of partially suspended individual single-walled carbon nanotubes," *Journal of Physical Chemistry C*, vol. 111, no. 5, pp. 1983–1987, 2007.

[38] J. C. Meyer, M. Paillet, T. Michel et al., "Raman modes of index-identified freestanding single-walled carbon nanotubes," *Physical Review Letters*, vol. 95, no. 21, Article ID 217401, pp. 1–4, 2005.

[39] H. Kataura, Y. Kumazawa, Y. Maniwa et al., "Optical properties of single-wall carbon nanotubes," *Synthetic Metals*, vol. 103, no. 1–3, pp. 2555–2558, 1999.

[40] P. T. Araujo, I. O. Maciel, P. B. C. Pesce et al., "Nature of the constant factor in the relation between radial breathing mode frequency and tube diameter for single-wall carbon

nanotubes," *Physical Review B*, vol. 77, no. 24, Article ID 241403, 2008.

[41] J. S. Soares, L. G. Cançado, E. B. Barros, and A. Jorio, "The Kataura plot for single wall carbon nanotubes on top of crystalline quartz," *Physica Status Solidi B*, vol. 247, no. 11-12, pp. 2835–2837, 2010.

[42] M. S. Dresselhaus, G. Dresselhaus, and M. Hofmann, "The big picture of Raman scattering in carbon nanotubes," *Vibrational Spectroscopy*, vol. 45, no. 2, pp. 71–81, 2007.

[43] P. T. Araujo, S. K. Doorn, S. Kilina et al., "Third and fourth optical transitions in semiconducting carbon nanotubes," *Physical Review Letters*, vol. 98, no. 6, Article ID 067401, 2007.

[44] S. K. Doorn, P. T. Araujo, K. Hata, and A. Jorio, "Excitons and exciton-phonon coupling in metallic single-walled carbon nanotubes: resonance Raman spectroscopy," *Physical Review B*, vol. 78, no. 16, Article ID 165408, 2008.

[45] P. T. Araujo, P. B. C. Pesce, M. S. Dresselhaus, K. Sato, R. Saito, and A. Jorio, "Resonance Raman spectroscopy of the radial breathing modes in carbon nanotubes," *Physica E*, vol. 42, no. 5, pp. 1251–1261, 2010.

[46] L. D. Machado, S. B. Legoas, J. S. Soares et al., "On the formation of carbon nanotube serpentines: insights from multi-million atom molecular dynamics simulation," *Materials Research Society Symposium Proceedings*, vol. 1284, pp. 79–84, 2011.

[47] S. B. Cronin, A. K. Swan, M. S. Ünlü, B. B. Goldberg, M. S. Dresselhaus, and M. Tinkham, "Measuring the uniaxial strain of individual single-wall carbon nanotubes: resonance Raman spectra of atomic-force-microscope modified single-wall nanotubes," *Physical Review Letters*, vol. 93, no. 16, p. 167401, 2004.

[48] X. Duan, H. Son, B. Gao et al., "Resonant Raman spectroscopy of individual strained single-wall carbon nanotubes," *Nano Letters*, vol. 7, no. 7, pp. 2116–2121, 2007.

[49] B. Gao, L. Jiang, X. Ling, J. Zhang, and Z. Liu, "Chirality-dependent Raman frequency variation of single-walled carbon nanotubes under uniaxial strain," *Journal of Physical Chemistry C*, vol. 112, no. 51, pp. 20123–20125, 2008.

[50] A. Das, A. K. Sood, A. Govindaraj et al., "Doping in carbon nanotubes probed by Raman and transport measurements," *Physical Review Letters*, vol. 99, no. 13, Article ID 136803, 2007.

[51] O. Dubay, G. Kresse, and H. Kuzmany, "Phonon softening in metallic nanotubes by a Peierls-like mechanism," *Physical Review Letters*, vol. 88, no. 23, pp. 2355061–2355064, 2002.

[52] J. C. Tsang, M. Freitag, V. Perebeinos, J. Liu, and P. Avouris, "Doping and phonon renormalization in carbon nanotubes," *Nature Nanotechnology*, vol. 2, no. 11, pp. 725–730, 2007.

[53] S. Piscanec, M. Lazzeri, J. Robertson, A. C. Ferrari, and F. Mauri, "Optical phonons in carbon nanotubes: kohn anomalies, Peierls distortions, and dynamic effects," *Physical Review B*, vol. 75, no. 3, Article ID 035427, 2007.

[54] I. O. MacIel, N. Anderson, M. A. Pimenta et al., "Electron and phonon renormalization near charged defects in carbon nanotubes," *Nature Materials*, vol. 7, no. 11, pp. 878–883, 2008.

[55] J. S. Soares, E. B. Barros, N. Shadmi, E. Joselevich, and A. Jorio, "Raman study of nanotube-substrate interaction using single-wall carbon nanotubes grown on crystalline quartz," *Physica Status Solidi*, vol. 248, no. 11, pp. 2536–2539, 2011.

[56] M. S. Dresselhaus, G. Dresselhaus, A. Jorio, A. G. Souza Filho, G. G. Samsonidze, and R. Saito, "Science and applications of single-nanotube raman spectroscopy," *Journal of Nanoscience and Nanotechnology*, vol. 3, no. 1-2, pp. 19–37, 2003.

[57] A. P. M. Barboza, A. P. Gomes, H. Chacham, and B. R. A. Neves, "Probing electric characteristics and sorting out metallic from semiconducting carbon nanotubes," *Carbon*, vol. 48, no. 11, pp. 3287–3292, 2010.

[58] Y. K. Kwon, S. Saito, and D. Tománek, "Effect of intertube coupling on the electronic structure of carbon nanotube ropes," *Physical Review B*, vol. 58, no. 20, pp. R13314–R13317, 1998.

[59] A. M. Rao, J. Chen, E. Richter et al., "Effect of van der Waals interactions on the Raman modes in single walled carbon nanotubes," *Physical Review Letters*, vol. 86, no. 17, pp. 3895–3898, 2001.

[60] S. Reich, C. Thomsen, and P. Ordejón, "Electronic band structure of isolated and bundled carbon nanotubes," *Physical Review B*, vol. 65, no. 15, p. 1554111, 2002.

[61] F. Villalpando-Paez, H. Muramatsu, Y. A. Kim et al., "Wall-to-wall stress induced in (6,5) semiconducting nanotubes by encapsulation in metallic outer tubes of different diameters: a resonance Raman study of individual C60-derived double-wall carbon nanotubes," *Nanoscale*, vol. 2, no. 3, pp. 406–411, 2010.